The medial axis of closed bounded sets is Lipschitz stable with respect to the Hausdorff distance under ambient diffeomorphisms

Hana Dal Poz Kouřimská, André Lieutier, Mathijs Wintraecken

The medial axis of closed bounded sets is Lipschitz stable with respect to the Hausdorff distance under ambient diffeomorphisms

Hana Dal Poz Kouřimská [1], André Lieutier[2], Mathijs Wintraecken[3]

[1]Edelsbrunner group, Institute of Science and Technology Austria, Am Campus 1, Klosterneuburg, 3400, Austria.
[2]No affiliation, Aix-en-Provence, France.
[3]Centre Inria d'Université Côte d'Azur, Université Côte d'Azur, Inria, 2004 Rte des Lucioles, Valbonne, 06902, France.

Contributing authors: hana.kourimska@ist.ac.at; andre.lieutier@gmail.com; mathijs.wintraecken@inria.fr;

Abstract

We prove that the medial axis of closed sets is Hausdorff stable in the following sense: Let $\boldsymbol{\mathcal{S}} \subseteq \mathbb{R}^{\boldsymbol{d}}$ be a fixed closed set that contains a bounding sphere. Consider the space of $\boldsymbol{C^{1,1}}$ diffeomorphisms of $\mathbb{R}^{\boldsymbol{d}}$ to itself, which keep the bounding sphere invariant. The map from this space of diffeomorphisms (endowed with a Banach norm) to the space of closed subsets of $\mathbb{R}^{\boldsymbol{d}}$ (endowed with the Hausdorff distance), mapping a diffeomorphism $\boldsymbol{F}$ to the closure of the medial axis of $\boldsymbol{F(\mathcal{S})}$, is Lipschitz.
This extends a previous stability result of Chazal and Soufflet on the stability of the medial axis of $\boldsymbol{C^2}$ manifolds under $\boldsymbol{C^2}$ ambient diffeomorphisms.

Keywords: Medial axis, Hausdorff distance, Lipschitz continuity

1 Introduction

In [1], Federer introduced the *reach* of a (closed) set $\mathcal{S} \subset \mathbb{R}^d$ as the infimum over all points in $\mathcal{S}$ of the distance from these points to the *medial axis* $\mathrm{ax}(\mathcal{S})$, the set of points in $\mathbb{R}^d$ for which the closest point in $\mathcal{S}$ is not unique. Federer also introduced the reach

at a point $p \in \mathcal{S}$ to be the distance from p to the medial axis of $\mathcal{S}$. We now call this quantity the *local feature size* [2] and denote it by $\mathrm{lfs}(p)$.

Federer proved that the reach is stable under $C^{1,1}$ diffeomorphisms of the ambient space. Here, a $C^{1,1}$ map is a C^1 map whose derivative is Lipschitz, and a $C^{1,1}$ diffeomorphism is a $C^{1,1}$ bijective map whose inverse is also $C^{1,1}$. Chazal and Soufflet [3] proved that the medial axis is stable with respect to the Hausdorff distance under ambient diffeomorphisms, but under stronger assumptions than the work of Federer, namely assuming that $\mathcal{S}$ is a C^2 manifold and the distortion is a C^2 diffeomorphism of the ambient space. Chazal and Soufflet based their work on earlier results by Blaschke [4], which were not as strong as Federer's.

In this paper we extend the stability result of the medial axis. More concretely, we generalize the result of Chazal and Soufflet [3] to arbitrary closed sets and $C^{1,1}$ diffeomorphisms of the ambient space; we show that the Hausdorff distance between the medial axes of the closed set and its image is bounded in terms of Lipschitz constants stemming from the diffeomorphism of the ambient space. Our result follows from the work of Federer [1] and in fact shortens the proof in [3] significantly.

Our bounds on the Hausdorff distance say nothing about the topology of the medial axis, which is known to be highly unstable (see e.g. [5]), although it preserves the homotopy type (see [6]).

Contribution and related work

Our work differs from the majority of the literature in three essential ways:

Firstly, we make no assumptions on the set we consider apart from that it is closed. The stability of the medial axis of (piecewise) smooth manifolds has been the object of intense study, see for example [3, 7–15]. However, the manifold assumption is impossible to achieve in many applications — such as in the context of astrophysics, one of the main motivations of this paper.

Secondly, we achieve stability without pruning the medial axis. This contrasts with a large body of work, such as [11, 16–18]. Not having to prune the medial axis is a significant advantage. On the downside, we limit the changes of the considered set to those induced by ambient diffeomorphisms. Nevertheless, given the standard examples of the instability of the medial axis — see for example [5] — we believe these limitations are near to the weakest assumptions necessary for Hausdorff stability. Within the context of ambient homeomorphisms, the results we obtain are close to optimal, as we specify in Remark 20.

Thirdly, our results hold for sets in arbitrary dimensions and are not sensitive to the dimension of the set itself. A large part of the related work only investigates sets of low dimensions or codimension one manifolds, although there are some notable exceptions such as [15], see also [13], and [17, 18].

Motivation

The medial axis has many real world applications — among others, in robot motion planning [19], triangulation algorithms [20], graphics [21], vision [22, 23], and shape recognition, segmentation, and learning [24–31]. See also the overviews [21, 32]. The

reach — the distance between a set and its medial axis — is a central concept in manifold learning [33–38].

The motivation of this paper is twofold: Firstly, we tackle the following challenge from the processing of images collected with optical devices which use lenses — such as cameras or telescopes: A shape extracted from such an image may be imprecise due to the imperfection of the lenses.

Our result implies that the medial axis of such a shape is stable under these imperfections. As a consequence, the outcome of any shape recognition or shape segmentation algorithm based on the medial axis will be stable.

In addition to the disciplines listed at the beginning of this paragraph, the stability of the medial axis is sought after in astrophysics, in particular for shape analysis and automated shape identification in observational astronomy. Observational astronomers are interested in reconstructing objects like stars or galaxies, and their place in the universe from data gathered by telescopes. They can deduce the distance from the object to the observer thanks to so-called standard candles or red shift [39–41]. However, the image gets distorted due to optical effects — either through gravitational lensing ([42]) or lensing inside the telescope itself ([43]).

Such a distortion can be modeled as a diffeomorphism of the ambient space. At the same time, this problem cannot be tackled using the result by Chazal and Soufflet [3], since the observed objects might not be smooth — for example due to interactions with shock waves or jets. In addition, with our method astrophysicists can not only reconstruct objects in space (3D), but also in spacetime (4D).

Another context where the removal of the assumption that the set is a (smooth) manifold, is important is biology; branching structures are ubiquitous in nature. In fact, it was questions from biology that motivated the 'introduction'[1] of the medial axis by Blum [46].

The second motivation is more formal in nature: The stability of the medial axis is instrumental in establishing its computability. Indeed, when proving properties of algorithms based on the medial axis, authors generally assume the real RAM model.[2] However, as was recently argued in [18], the medial axis needs to be stable in order to be computable in more realistic models of computation.

There is a more practical component to this formal question: It is not a priori clear if using possibly noisy real world data or the output of other computer programs as input for these algorithms yields answers that are close to the ground truth. To be able to prove that the output is correct, we need (numerical) stability of the medial axis.

Outline

After revisiting preliminaries and known results in Section 2, we state the main stability result in Section 3. In Section 4 we reformulate this result in terms of norms on Banach spaces. This also exhibits the fact that the stability of the medial axis is Lipschitz in the following sense: We think of the set $\mathcal{S}$ as fixed and consider the map from the space of diffeomorphisms (endowed with a norm which makes it a Banach

[1] The medial axis was studied before by Erdős [44, 45] in a different context.

[2] The real RAM model is a standard, albeit non-realistic, assumption in Computational Geometry. It assumes one can calculate precisely with real numbers, instead of using 0s and 1s (which is the usual assumption in computer science).

space) to the space of closed subsets of $\mathbb{R}^d$ (endowed with the Hausdorff distance), mapping each diffeomorphism $F : \mathbb{R}^d \to \mathbb{R}^d$ to the closure of the medial axis of $F(\mathcal{S})$. The Lipschitz constant then only depends on the diameter of the bounding sphere of the set $\mathcal{S}$. We conclude with some future work.

2 Preliminaries: Sets of positive reach and the closest point projection

In this section we recall some definitions and results concerning the medial axis and sets of positive reach. Essentially, we need three ingredients from the literature to prove our main theorem: the notions related to the closest point projection, the properties of the generalized normal and tangent spaces, and Federer's result on the stability of the reach under ambient diffeomorphisms.

We write $d(\cdot, \cdot)$ for the Euclidean distance between two points, and the distance between a point and a set. That is, for any closed set $\mathcal{S}$ and point p,

$$d(p, \mathcal{S}) = \inf_{q \in \mathcal{S}} d(p, q).$$

We denote the Hausdorff distance between two sets $A, B \subseteq \mathbb{R}^d$ by $d_H(A, B)$:

$$d_H(A, B) = \max \left\{ \sup_{a \in A} d(a, B), \sup_{b \in B} d(b, A) \right\}.$$

We write $B(c, r)$, resp. $S(c, r)$, to denote balls, resp. spheres, with centre c and radius r. Lastly, $|\cdot|$ denotes the Euclidean norm, and $\|\cdot\|$ an operator norm.

The closest point projection and related notions

The projection of points in the ambient space $\mathbb{R}^d$ to the (set of) closest point(s) of the set $\mathcal{S} \subseteq \mathbb{R}^d$ is denoted by $\pi_{\mathcal{S}}$, and illustrated in Figure 1.

The *medial axis* of $\mathcal{S}$ is the set of all points $p \in \mathbb{R}^d$ where the set $\pi_{\mathcal{S}}(p)$ consists of more than one point:

$$\operatorname{ax}(\mathcal{S}) = \left\{ p \in \mathbb{R}^d \mid \#\pi_{\mathcal{S}}(p) > 1 \right\}.$$

Here, $\#\pi_{\mathcal{S}}(p)$ denotes the cardinality of the set $\pi_{\mathcal{S}}(p)$.

For a point $p \in \mathcal{S}$, the *local feature size of* p is the distance from p to the medial axis of the set $\mathcal{S}$:

$$\operatorname{lfs}(p) = d(p, \operatorname{ax}(\mathcal{S})).$$

Finally, the *reach* of the set $\mathcal{S}$ is the infimum of the local feature size over all its points:

$$\operatorname{rch}(\mathcal{S}) = \inf_{p \in \mathcal{S}} \operatorname{lfs}(p) = \inf_{p \in \mathcal{S}} d(p, \operatorname{ax}(\mathcal{S})).$$

Throughout this paper we assume that $\mathcal{S} \subseteq \mathbb{R}^d$ is a closed set. We shall further assume that the set $\mathcal{S}$ as well as its medial axis are bounded, and that the bounding sphere of $\mathcal{S}$ is contained in $\mathcal{S}$ itself. More specifically, we assume that there

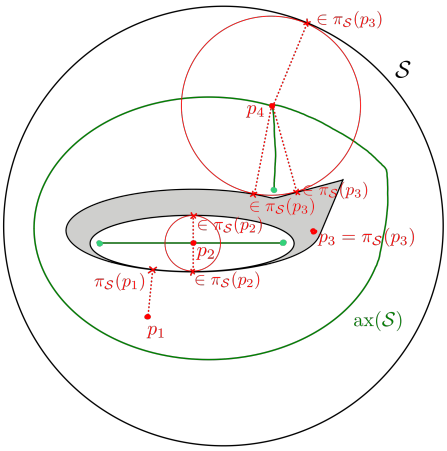

Fig. 1 The closest point projection to the set $\mathcal{S}$ of four points in $\mathbb{R}^2$. When a point lies on the medial axis $\mathrm{ax}(\mathcal{S})$, the closest point projection consists of more points.

exists a closed ball B of positive radius such that $\mathcal{S} \subseteq B$, and $\partial B \subseteq \mathcal{S}$. We call ∂B the bounding sphere of $\mathcal{S}$.

The addition of the bounding sphere ∂B to the set $\mathcal{S}$ is necessary to obtain the desired bound on the Hausdorff distance between the two medial axes of the set $\mathcal{S}$ and its image under the ambient diffeomorphism. Indeed, consider the following example, illustrated in Figure 2.

Let the set $\mathcal{S}$ consist of two points in the plane, $\mathcal{S} = \{p, q\} \subseteq \mathbb{R}^2$. The medial axis of $\mathcal{S}$ is then the bisector line of p and q. After a generic perturbation F of p and q — that is, not a translation and not a perturbation in the direction $\pm(p - q)$ — the bisector line $\mathrm{ax}(F(\mathcal{S}))$ of the perturbed points intersects the bisector $\mathrm{ax}(\mathcal{S})$ of the original pair. The Hausdorff distance between these two non-parallel lines is infinite, and thus unboundable. If, however, we restrict ourselves to a ball around the origin of size r, the Hausdorff distance between the two restricted medial axes is of order $\mathcal{O}(r\theta)$, where θ is the angle between the vectors $p - q$ and $F(p) - F(q)$.

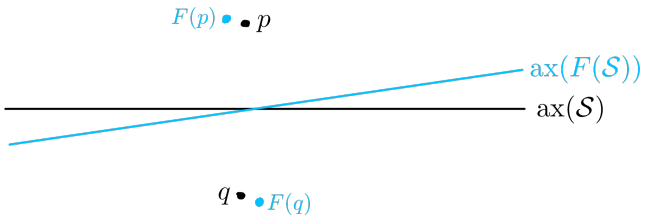

Fig. 2 In black the set $\mathcal{S}$ and its medial axis, in light blue the perturbed set and its medial axis. Since the lines $\mathrm{ax}(\mathcal{S})$ and $\mathrm{ax}(F(\mathcal{S}))$ are non-parallel, the Hausdorff distance between them is infinite. Hence it is impossible to give a bound on the distance between the medial axes without localizing.

At the same time, the addition of the bounding sphere ∂B to the considered set $\mathcal{S}$ is not a restriction. Indeed,

Remark 1. *The medial axes of $\mathcal{S}$ and $\mathcal{S} \setminus \partial B$ coincide in the interior of the ball B sufficiently far away from its boundary ∂B. More precisely:*

- *Any point $x \in \operatorname{ax}(\mathcal{S})$, such that $\pi_{\mathcal{S}}(x) \cap \partial B = \emptyset$, lies on the medial axis $\operatorname{ax}(\mathcal{S} \setminus \partial B)$.*
- *Conversely, if a point x lies on the medial axis $\operatorname{ax}(\mathcal{S} \setminus \partial B)$, and any (and thus every) point $q \in \pi_{\mathcal{S} \setminus \partial B}(x)$ satisfies $d(x, q) < d(x, \partial B)$, then $x \in \operatorname{ax}(\mathcal{S})$.*

Thus, the medial axis is locally stable if the ambient diffeomorphism is close to the identity.[3]

A recurring strategy in this article is to start at a point p on the set $\mathcal{S}$, move away from this point in a 'normal' direction, and see if by projecting using the closest point projection $\pi_{\mathcal{S}}$ we get back to p. To this end, we define the *projection range*.

Definition 2 (Projection range)**.** *Let $p \in \mathcal{S}$ be a point and $v \in \mathbb{R}^d$ a vector. The* projection range $d(p, v, \pi_{\mathcal{S}})$ *in direction v is the maximal distance one can travel from p along v such that the closest point projection yields only the point p:*

$$d(p, v, \pi_{\mathcal{S}}) = \sup\{\lambda \in \mathbb{R} \mid \pi_{\mathcal{S}}(p + \lambda v) = \{p\}\}.$$

Since $\pi_{\mathcal{S}}(p) = \{p\}$, the projection range is canonically non-negative. Furthermore, the directions for which the range is positive are key to our study, because of the following property:

Lemma 3 (Theorem 4.8 (6) of [1])**.** *Consider a point $p \in \mathcal{S}$ and a vector $v \in \mathbb{R}^d$. If*

$$0 < d(p, v, \pi_{\mathcal{S}}) < \infty,$$

then $p + d(p, v, \pi_{\mathcal{S}}) \cdot v \in \overline{\operatorname{ax}(\mathcal{S})}$.

We call these special directions v *back projection vectors*:

Definition 4 (Unit back projection vectors)**.** *For a point $p \in \mathcal{S}$,* $\operatorname{UBP}(p, \mathcal{S})$ *is the set of unit vectors with a positive projection range:*

$$\operatorname{UBP}(p, \mathcal{S}) = \left\{u \in \mathbb{R}^d \mid |u| = 1 \text{ and } 0 < d(p, u, \pi_{\mathcal{S}}) < \infty\right\}.$$

We further define

$$\operatorname{UBP}(\mathcal{S}) = \left\{(p, u) \in \mathcal{S} \times \mathbb{R}^d \,\middle|\, u \in \operatorname{UBP}(p, \mathcal{S})\right\},$$
$$\operatorname{BP}(\mathcal{S}) = \left\{(p, \lambda u) \in \mathcal{S} \times \mathbb{R}^d \,\middle|\, (p, u) \in \operatorname{UBP}(\mathcal{S}), \lambda \geq 0\right\}.$$

Thanks to Lemma 3, the following map is well-defined:

$$\pi_{\operatorname{ax},\mathcal{S}} : \operatorname{UBP}(\mathcal{S}) \to \overline{\operatorname{ax}(\mathcal{S})}, \qquad (p, u) \mapsto p + d(p, u, \pi_{\mathcal{S}})u. \tag{1}$$

[3] The bounding sphere does allow one to give a relatively clean mathematical statement, see Section 4.

The generalized tangent and normal space

Back projection vectors are intricately related to the generalized tangent and normal spaces.

Definition 5 (Definitions 4.3 and 4.4 of [1]). *Let $p \in \mathcal{S}$. The* generalized tangent space $\mathrm{Tan}(p, \mathcal{S})$ *is the set of vectors $u \in \mathbb{R}^d$, such that either $u = 0$ or, for every $\varepsilon > 0$ there exists a point $q \in \mathcal{S}$ with*

$$0 < |q - p| < \varepsilon \qquad \text{and} \qquad \left| \frac{q-p}{|q-p|} - \frac{u}{|u|} \right| < \varepsilon.$$

The generalized normal space $\mathrm{Nor}(p, \mathcal{S})$ *consists of vectors $v \in \mathbb{R}^d$ such that $\langle v, u \rangle \leq 0$ for all $u \in \mathrm{Tan}(p, \mathcal{S})$. Vectors contained in the generalized tangent, resp. normal, space are called* tangent, *resp.* normal, to $\mathcal{S}$ at p.

The generalized tangent and normal spaces are illustrated in Figure 3.

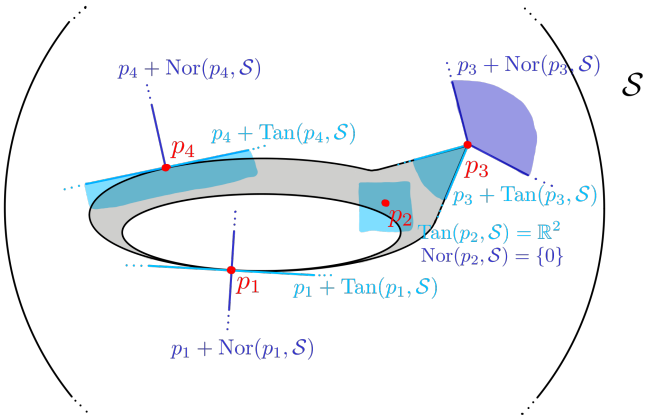

Fig. 3 The (affine) generalized tangent and normal spaces of four points in the set $\mathcal{S} \subset \mathbb{R}^2$, in light blue and violet, respectively.

Stability of the reach under ambient diffeomorphisms

Our last ingredient is the following result by Federer.

Theorem 6 (Stability of the reach under ambient diffeomorphisms, Theorem 4.19 of [1]). *Pick two constants $0 < t < \mathrm{rch}(\mathcal{S})$ and $s > 0$. If the map*

$$F : \{x \in \mathbb{R}^d \mid d(x, \mathcal{S}) < s\} \to \mathbb{R}^n$$

is injective and continuously differentiable, and the maps F, F^{-1}, and DF are Lipschitz continuous with Lipschitz constants $\mathrm{Lip}(F)$, $\mathrm{Lip}(F^{-1})$, $\mathrm{Lip}(DF)$, *respectively,*

then the reach $\operatorname{rch}(F(\mathcal{S}))$ *of the image of the set* $\mathcal{S}$ *under the map* F *is lower-bounded by*

$$\operatorname{rch}(F(\mathcal{S})) \geq \min\left\{ \frac{s}{\operatorname{Lip}(F^{-1})}, \frac{1}{\left(\frac{\operatorname{Lip}(F)}{t} + \operatorname{Lip}(DF)\right)\left(\operatorname{Lip}(F^{-1})\right)^2} \right\}.$$

3 Stability of the medial axis under ambient diffeomorphisms

In this section we present the main result of this paper, Theorem 18. This theorem extends earlier work by Chazal and Soufflet [3]. Its proof relies on Federer's result on the stability of the reach, Theorem 6. To give a more geometrical interpretation we introduce the concept of a weakly tangent sphere and ball, and a maximal empty weakly tangent ball.

Definition 7 (Weakly tangent sphere and ball)**.** *Let* $p \in \mathcal{S}$*. A sphere is called* weakly tangent to $\mathcal{S}$ at p *if it contains the point* p *and its centre lies in the (translated) generalized normal space* $\operatorname{Nor}(p, \mathcal{S}) + p$*. In other words, spheres weakly tangent to* $\mathcal{S}$ *at* p *are spheres with centres* $p + v$ *and radii* $|v|$*, for a vector* $v \in \operatorname{Nor}(p, \mathcal{S})$*.*

A ball is called weakly tangent to $\mathcal{S}$ at p *if its boundary sphere is* weakly tangent to $\mathcal{S}$ at p*.*

Remark 8. *Using the definition of* $\operatorname{Nor}(p, \mathcal{S})$*, a weakly tangent ball can also be defined as follows: A ball* $B(c, r)$ *is weakly tangent at* p *if and only if its centre* c *and radius* r *satisfy*

$$(p + \operatorname{Tan}(\mathcal{S}, p)) \cap B(c, r) = \{p\}.$$

We further remark:

Lemma 9. *Let* $p \in \mathcal{S}$ *and* $v \in \mathbb{R}^d$*, and suppose that for some* $\lambda > 0$ *we have* $\pi_{\mathcal{S}}(p + \lambda v) \neq \{p\}$*. Then, for all* $\lambda' \geq \lambda$*, we have* $\pi_{\mathcal{S}}(p + \lambda' v) \neq \{p\}$ *and for all* $\lambda' > \lambda$*, that* $p \notin \pi_{\mathcal{S}}(p + \lambda' v)$*.*

Proof. We first note that the statement is empty if $v = 0$. Let $v \neq 0$, and consider the nested family of balls $B(p + \lambda' v, \lambda' |v|)$, parametrized by $\lambda' > 0$.

Because $\pi_{\mathcal{S}}(p + \lambda v) \neq p$, the (closed) ball $B(p + \lambda v, \lambda |v|)$ contains a point $q \in \mathcal{S}$ other than p. Since the balls $B(p + \lambda' v, \lambda' |v|)$ are nested, the point q lies inside every ball $B(p + \lambda' v, \lambda' |v|)$ with $\lambda' \geq \lambda$. Moreover, q lies in the interior of $B(p + \lambda' v, \lambda' |v|)$ for $\lambda' > \lambda$. Hence, for every $\lambda' \geq \lambda$, we have that $\pi_{\mathcal{S}}(p + \lambda' v) \neq \{p\}$ and for $\lambda' > \lambda$, that $p \notin \pi_{\mathcal{S}}(p + \lambda' v)$. □

Lemma 9 essentially tells us that a family of weakly tangent balls $\{B(p + \lambda v, \lambda |v|)\}_{\lambda \geq 0}$ contains at most one which is maximal with respect to inclusion among those whose interior is disjoint from the set $\mathcal{S}$. Two such families are illustrated in Figure 4.

We call such balls *maximal empty*. For the purpose of this article, we define maximal empty balls in terms of unit back projection vectors (Definition 4). To see that each maximal empty ball is indeed weakly tangent, we emphasise:

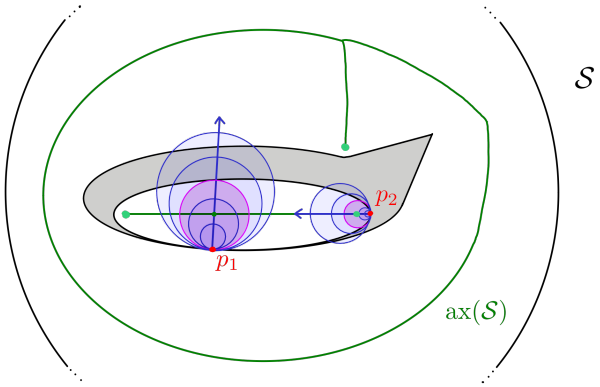

Fig. 4 Two families of balls weakly tangent to the set $\mathcal{S} \subset \mathbb{R}^2$ (in blue). Each family contains a unique maximal empty ball (in purple). Notice that the centre of the maximal empty ball weakly tangent at the point p_1 lies at the medial axis $\mathrm{ax}(\mathcal{S})$, while the centre of the maximal empty ball weakly tangent at the point p_2 only lies at its closure, $\overline{\mathrm{ax}(\mathcal{S})}$.

Lemma 10. *If $(p, v) \in \mathrm{BP}(\mathcal{S})$, then $(p, v) \in \mathrm{Nor}(\mathcal{S})$. That is, $\mathrm{BP}(\mathcal{S}) \subseteq \mathrm{Nor}(\mathcal{S})$. In particular, for any pair $(p, u) \in \mathrm{UBP}(\mathcal{S})$ and radius $\lambda \geq 0$, the ball $B(p + \lambda u, \lambda)$ is weakly tangent to $\mathcal{S}$.*

Remark 11. *For general closed sets, the converse of Lemma 10, that is, $\mathrm{Nor}(\mathcal{S}) \subseteq \mathrm{BP}(\mathcal{S})$, is not true. One counter-example is the graph of the function $x \mapsto |x|^{3/2}$ at the origin. However, the inclusion $\mathrm{Nor}(\mathcal{S}) \subseteq \mathrm{BP}(\mathcal{S})$ holds for sets of positive reach thanks to [1, Theorem 4.8 (12)], which we recall as Lemma 22 in the appendix.*

Definition 12 (Maximal empty weakly tangent ball)**.** *Let $(p, u) \in \mathrm{UBP}(\mathcal{S})$. A weakly tangent ball $B(p + \lambda u, \lambda)$ is called* maximal empty *to $\mathcal{S}$ if $\lambda = d(p, u, \pi_{\mathcal{S}})$, or, equivalently, if $\pi_{\mathrm{ax},\mathcal{S}}(p, u) = p + \lambda u$.*

(Maximal empty) weakly tangent balls satisfy the following properties. Let $(p, u) \in \mathrm{UBP}(\mathcal{S})$.

- For any radius $0 < \lambda \leq d(p, u, \pi_{\mathcal{S}})$, the interior of the ball $B(p + \lambda u, \lambda)$ is disjoint from the set $\mathcal{S}$. This follows directly from Definition 12 and Lemma 9.
- The centres of maximal empty weakly tangent balls lie on the closure of the medial axis of $\mathcal{S}$. This is due to Lemma 3 and the definition of the map $\pi_{\mathrm{ax},\mathcal{S}}$ (equation (1)).

The following lemma moreover tells us, that each point on the medial axis is a centre of a maximal empty weakly tangent ball.

Lemma 13 (Surjectivity on $\mathrm{ax}(\mathcal{S})$)**.** *For any point $x \in \mathrm{ax}(\mathcal{S})$ and $p \in \pi_{\mathcal{S}}(x)$, there exists a vector $u \in \mathrm{UBP}(p, \mathcal{S})$ such that $\pi_{\mathrm{ax},\mathcal{S}}(p, u) = x$. In other words, $B(x, |x - p|)$ is a maximally empty weakly tangent ball. Moreover, we have that*

$$\mathrm{ax}(\mathcal{S}) \subseteq \pi_{\mathrm{ax},\mathcal{S}}\left(\mathrm{UBP}(\mathcal{S})\right) \subseteq \overline{\mathrm{ax}(\mathcal{S})}.$$

Proof. Let $Q = \pi_{\mathcal{S}}(x)$ be the subset of $\mathcal{S}$ that is closest to x. Because $x \in \mathrm{ax}(\mathcal{S})$, Q contains at least two points, one of them being p. We write $\lambda = |x - p|$. Since $\mathcal{S}$ and $\mathrm{ax}(\mathcal{S})$ are disjoint, $\lambda > 0$, and thus we can define $u = \frac{x-p}{\lambda}$.

Since the interior of the ball $B(x,\lambda)$ does not intersect $\mathcal{S}$, it in particular does not intersect $\mathrm{Tan}(p,\mathcal{S})$ and thus $B(x,\lambda)$ is weakly tangent at p by Remark 8. Let us now consider the nested family $B(p+\lambda' u,\lambda')$ of weakly tangent balls at p. By definition, $\partial B(x,\lambda)\cap\mathcal{S} = Q$ and therefore $B(p+\lambda' u,\lambda')\cap\mathcal{S} = p$ for $\lambda' < \lambda$. At the same time, Lemma 9 yields that for $\lambda' > \lambda$, $p \notin \pi_{\mathcal{S}}(p+\lambda' u)$. Hence the projection range in direction u equals $d(p,u,\pi_{\mathcal{S}}) = \lambda$ and we obtain $\pi_{\mathrm{ax},\mathcal{S}}(p,u) = p+\lambda u = x$ directly from Definition 12 . The fact that $\pi_{\mathrm{ax},\mathcal{S}}\left(\mathrm{UBP}(\mathcal{S})\right) \subseteq \overline{\mathrm{ax}(\mathcal{S})}$ is due to Lemma 3. □

We are now almost ready to state our main theorem. Before phrasing the result, we walk the reader through the assumptions and fix the notation on the way. The assumptions are illustrated in Figure 5.

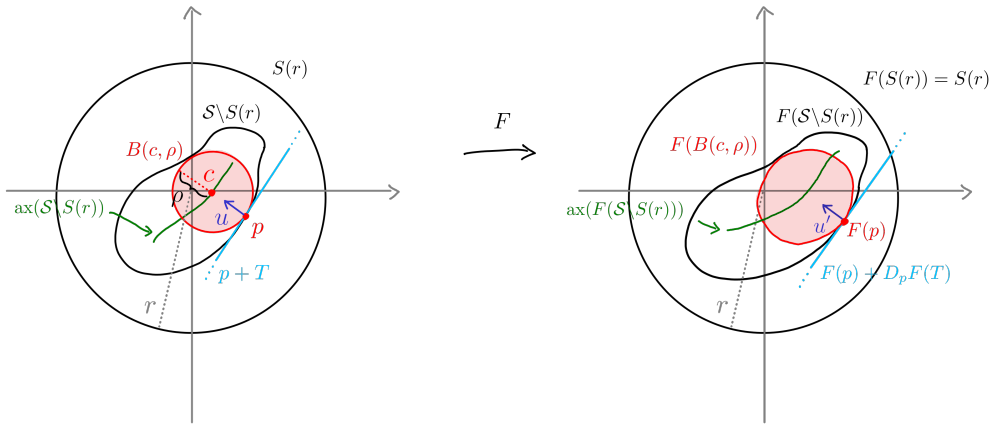

Fig. 5 The setting of Theorem 18.

Assumption 14.

- *We assume that the set $\mathcal{S}$ has a bounding sphere of radius r, which we denote by $S(r)$.*
- *We consider a C^1 diffeomorphism $F:\mathbb{R}^d\to\mathbb{R}^d$ such that the Lipschitz constants of F and F^{-1} are bounded by L_F, and the Lipschitz constants of the differentials DF and DF^{-1} are bounded by L_{DF}. We call such a diffeomorphism a $C^{1,1}$ diffeomorphism.*
- *We further assume that the map F leaves the bounding sphere $S(r)$ invariant, that is, $F(S(r)) = S(r)$.*
- *We pick a point $c\in\mathrm{ax}(\mathcal{S})$, a point $p\in\pi_{\mathcal{S}}(c)$, and write $\rho = |c-p|$. Observe that since $\mathcal{S}\cap\mathrm{ax}(\mathcal{S}) = \emptyset$, ρ is positive. By Lemma 13, the ball $B(c,\rho)$ is a maximal empty weakly tangent ball to $\mathcal{S}$ at p. Moreover, we define $u = \frac{c-p}{|c-p|}$ and note that $u\in\mathrm{UBP}(p,\mathcal{S})$.*
- *We denote the tangent hyperplane to the boundary sphere of $B(c,\rho)$ at p by $p+T$. The hyperplane T is the orthocomplement of the vector u: $T = u^{\perp}$.*

- *We work with the unit vector at $F(p)$ that points inside the image of the ball $B(c,\rho)$ and is orthogonal to the hyperplane $D_pF(T)$. We denote this vector by u'.*

Remark 15. *Thanks to Remark 1, the first and the third assumption can be replaced by the following:*

- *As assumption on the density of $\mathcal{S}$: Every point in $\mathbb{R}^d$ is at most a distance r from a point in $\mathcal{S}$, and this property is preserved by F.*
- *We do not have to explicitly refer to the bounding sphere. That is, our bounds hold for any ball $B(c,r/2)$ satisfying $B(c,r/2-L_Fr)\cap\mathcal{S}\neq\emptyset$.*

The following properties of u and u' play an important rule in the proof of the theorem:

Claim 16.

$$u' = \frac{(D_pF^t)^{-1}(u)}{|(D_pF^t)^{-1}(u)|}, \tag{2}$$

where D_pF^t is the transpose matrix (or the adjoint operator) of DF at the point p, defined by

$$\forall v_1, v_2, \qquad \langle v_1, D_pF(v_2)\rangle = \langle D_pF^t(v_1), v_2\rangle.$$

Claim 17. *Let $\|D_pF - \mathrm{Id}\,\| \le \varepsilon < 1$. Then the angle $\angle u,u'$ between the vectors u and u' satisfies*

$$\cos\angle u,u' \ge \sqrt{1-\varepsilon^2}.$$

The proof of both of these properties is an exercise in linear algebra, which we defer to the appendix.

Theorem 18. *Under the above assumptions, there exists a maximal empty weakly tangent ball $B(c',\rho')$ to the set $F(\mathcal{S})$, whose boundary sphere has an internal normal u'. In particular, the ball $B(c',\rho')$ is tangent to the affine hyperplane $F(p)+D_pF(T)$. Its radius ρ' is bounded by $\rho' \in \left[\frac{\rho}{(L_F)^3+\rho L_{DF}(L_F)^2}, \frac{(L_F)^3\rho}{1-\rho L_{DF}(L_F)^2}\right]$. Assume, moreover, that the distortions of both F and DF are bounded, that is, for all $x\in\mathbb{R}^d$,*

$$|F(x)-x| \le \varepsilon_1, \qquad \|DF_x - \mathrm{Id}\,\| \le \varepsilon_2 < 1, \tag{3}$$

and $r\cdot L_{DF}(L_F)^2 \le 1/2$. Define

$$C_L(r,L_F,L_{DF},\varepsilon_1,\varepsilon_2) = \\ 2r\sqrt{1+(L_F)^6\left(1+4rL_{DF}(L_F)^2\right)^2 - 2(L_F)^3\left(1+4rL_{DF}(L_F)^2\right)\sqrt{1-(\varepsilon_2)^2}} + \varepsilon_1$$

then the map $\pi_{\mathrm{ax},\mathcal{S}}$ satisfies

$$|\pi_{\mathrm{ax},\mathcal{S}}(p,u) - \pi_{\mathrm{ax},F(\mathcal{S})}(F(p),u')| \le C_L(r,L_F,L_{DF},\varepsilon_1,\varepsilon_2).$$

Thus, the Hausdorff distance between the medial axes of $\mathcal{S}$ and its image $F(\mathcal{S})$ is bounded by

$$d_H(\mathrm{ax}(\mathcal{S}), \mathrm{ax}(F(\mathcal{S}))) \leq C_L(r, L_F, L_{DF}, \varepsilon_1, \varepsilon_2). \tag{4}$$

The bound $|F(x) - x| \leq \varepsilon_1$ really is necessary, because we want our theorem to accommodate for rotations and translations, which rotate and translate the medial axis without changing distances and hence have Lipschitz constant 1. We further stress that if the diffeomorphism F is close to the identity, its Lipschitz constant satisfies $L_F \geq 1$, because by assumption F leaves the bounding sphere $S(r)$ invariant, and L_{DF} is close to zero.

Proof. We first derive the bounds for the radius ρ'. As the first step, we apply Theorem 6 to the boundary sphere $S(c, \rho)$ of the maximal empty weakly tangent ball $B(c, \rho)$. In particular, we can choose the constant s in Theorem 2.6arbitrarily large, and the constant t arbitrarily close to the reach $\mathrm{rch}(S(c, \rho)) = \rho$, to obtain:

$$\mathrm{rch}\left(F(S(c, \rho))\right) \geq \frac{1}{\left(\frac{L_F}{\rho} + L_{DF}\right)(L_F)^2} = \frac{\rho}{(L_F)^3 + \rho L_{DF}(L_F)^2} =: \rho_1.$$

This means that no open ball of radius ρ_1 tangent to the set $F(S(c, \rho))$ actually intersects $F(S(c, \rho))$. In addition, since the set $F(B(c, \rho))$ does not contain any points of $F(\mathcal{S})$ in its interior, no ball of radius ρ_1 that is tangent to $F(S(c, \rho))$ and whose centre lies inside $F(S(c, \rho))$ contains any point of $F(\mathcal{S})$.

The unit vector $u' \in DF_p(T)^\perp$ (defined in (2)) is defined such that the point $F(p) + \rho_1 u'$ lies inside the distorted ball $F(B(c, \rho))$. Due to the above observation, the ball $B(F(p) + \rho_1 u', \rho_1)$ is weakly tangent to $F(\mathcal{S})$ at $F(p)$ and contains no points of $F(\mathcal{S})$ in its interior.

Let us now consider the weakly tangent ball $B(F(p) + \rho'' u', \rho'')$, whose radius ρ'' satisfies

$$\rho'' > \frac{(L_F)^3 \rho}{1 - \rho L_{DF}(L_F)^2} =: \rho_2.$$

To shorten the notation, we set

$$F(p) + \rho'' u' =: c''.$$

To derive a contradiction, we assume that $B(c'', \rho'')$ is maximal empty. This is equivalent to assuming that $\mathrm{int} B(c'', \rho'') \cap F(\mathcal{S}) = \emptyset$, and thus $B(c'', \rho'')$ is a maximal empty weakly tangent ball to $F(p)$. Similarly to the beginning of the proof, we now apply Theorem 6 to the map F^{-1} and the boundary sphere $S(c'', \rho'') = \partial B(c'', \rho'')$. As a result, the reach of $F^{-1}(S(c'', \rho''))$ is at least

$$\mathrm{rch}\left(F^{-1}(S(c'', \rho''))\right) \geq \frac{\frac{(L_F)^3 \rho}{1 - \rho L_{DF}(L_F)^2}}{(L_F)^3 + \frac{(L_F)^3 \rho}{1 - \rho L_{DF}(L_F)^2} L_{DF}(L_F)^2} = \rho.$$

We conclude that there exists a ball that is tangent to the set $F^{-1}(S(c'', \rho''))$ at $F^{-1}(F(p)) = p$, whose radius is larger than ρ, and that does not contain any points of $\mathcal{S}$ in its interior. This contradicts the fact that the ball $B(c, \rho)$ is maximal empty, and completes the proof of the first part of the statement.

We now prove the bounds on the distortion of the map $\pi_{\mathrm{ax},\mathcal{S}}$. Let $\rho' \in [\rho_1, \rho_2]$ be the radius of the maximal empty weakly tangent ball at $F(p)$ in the direction u', and write $c' := F(p) + \rho' u'$ for its centre. We stress that, as a consequence of Lemma 3 (Theorem 4.8 (6) of [1]) , $c' \in \overline{\mathrm{ax}(F(\mathcal{S}))}$, but it is not necessarily true that $c' \in \mathrm{ax}(F(\mathcal{S}))$.

The goal is to estimate the distance between the two centres $c = \pi_{\mathrm{ax},\mathcal{S}}(p, u)$ and $c' = \pi_{\mathrm{ax},\mathcal{S}}(F(p), u')$. Indeed, since $c - p = \rho u$ and $c' - F(p) = \rho' u'$,

$$\begin{aligned} |c - c'| &= |c - p + p - F(p) + F(p) - c'| = |\rho u + p - F(p) - \rho' c'| \\ &\leq |\rho u - \rho' u'| + |F(p) - p| \,. \end{aligned}$$

Due to the assumptions of the theorem,$|F(p) - p| \leq \varepsilon_1$. Furthermore, thanks to Claim 17,

$$|\rho u - \rho' u'|^2 = \rho^2 + (\rho')^2 - 2\rho\rho' \cos \angle u, u' \leq \rho^2 + (\rho')^2 - 2\rho\rho' \sqrt{1 - (\varepsilon_2)^2}.$$

Recalling that $\rho' \in [\rho_1, \rho_2]$, we thus obtain

$$\begin{aligned} |\rho u - \rho' u'| &\leq \max\left(\sqrt{\rho^2 + (\rho_1)^2 - 2\rho\,\rho_1 \cos(\arcsin(\varepsilon_2))}, \sqrt{\rho^2 + (\rho_2)^2 - 2\rho\,\rho_2 \cos(\arcsin(\varepsilon_2))} \right) \\ &= \max\left(\sqrt{\rho^2 + (\rho_1)^2 - 2\rho\,\rho_1 \sqrt{1 - (\varepsilon_2)^2}}, \sqrt{\rho^2 + (\rho_2)^2 - 2\rho\,\rho_2 \sqrt{1 - (\varepsilon_2)^2}} \right). \end{aligned}$$

Hence,

$$|c - c'| \leq \max\left(\sqrt{\rho^2 + (\rho_1)^2 - 2\rho\,\rho_1 \sqrt{1 - (\varepsilon_2)^2}}, \sqrt{\rho^2 + (\rho_2)^2 - 2\rho\,\rho_2 \sqrt{1 - (\varepsilon_2)^2}} \right) + \varepsilon_1. \tag{5}$$

As the last step, we simplify the expression (5) (at the cost of weakening the bounds). For this, we assume that $\rho L_{DF} (L_F)^2 \leq 1/2$, so that

$$\rho_1 = \frac{\rho}{(L_F)^3 + \rho L_{DF} (L_F)^2} \geq \frac{\rho}{(L_F)^3} \left(1 - \rho \frac{L_{DF}}{L_F} \right), \tag{6}$$

$$\rho_2 = \frac{(L_F)^3 \rho}{1 - \rho L_{DF} (L_F)^2} \leq \rho (L_F)^3 \left(1 + 2\rho L_{DF} (L_F)^2 \right), \tag{7}$$

where we used that, for $x \in [0, 1/2]$, $\frac{1}{1+x} \geq 1 - x$ and $\frac{1}{1-x} \leq 1 + 2x$. We note that both ρ_1 and ρ_2 tend to ρ as L_F tends to 1 and L_{DF} tends to 0. We now consider $|\rho_1 - \rho|$ and $|\rho_2 - \rho|$, and claim that

$$|\rho_1 - \rho|, |\rho_2 - \rho| \leq \rho (L_F)^3 \left(1 + 2\rho L_{DF} (L_F)^2 \right) - \rho.$$

For $|\rho_2 - \rho| = \rho_2 - \rho$, the claim holds thanks to (7). To establish this for $|\rho_1 - \rho|$ requires a small calculation:

$$\begin{aligned}
|\rho_1 - \rho| = \rho - \rho_1 &\leq \rho - \frac{\rho}{(L_F)^3}\left(1 - \rho\frac{L_{DF}}{L_F}\right) && \text{(due to (6))} \\
&\leq \rho(L_F)^3\left(1 + 2\rho L_{DF}(L_F)^2\right) - \rho && \text{(assuming the claim holds)} \\
2\rho &\leq \rho(L_F)^3\left(1 + 2\rho L_{DF}(L_F)^2\right) + \frac{\rho}{(L_F)^3}\left(1 - \rho\frac{L_{DF}}{L_F}\right) \\
&&& \text{(reformulating the previous inequality)} \\
2 &\leq (L_F)^3 + \frac{1}{(L_F)^3} + 2\rho L_{DF}(L_F)^5 - \rho\frac{L_{DF}}{(L_F)^4},
\end{aligned}$$

where the final inequality holds because $x^3 + x^{-3} \geq 2$, and $2x^5 - x^{-4} \geq 0$, for $x \geq 1$. We now consider the function

$$\begin{aligned}
f(\delta) &= \rho^2 + \rho^2(1+\delta)^2 - 2\rho^2(1+\delta)\sqrt{1-(\varepsilon_2)^2} \\
&= \rho^2\left(\delta^2 + 2\left(1 - \sqrt{1-(\varepsilon_2)^2}\right)\delta + 2\left(1 - \sqrt{1-(\varepsilon_2)^2}\right)\right).
\end{aligned}$$

The function f is a second order polynomial in δ and because all coefficients are positive, the maximum of f on the interval $[-\delta_m, \delta_m]$ is a attained at δ_m, that is,

$$\sup_{\delta\in[-\delta_m,\delta_m]} f(\delta) = f(\delta_m).$$

By combining these results, we see that

$$\begin{aligned}
&|c - c'| \\
&\leq \sqrt{f\left((L_F)^3\left(1 + 2\rho L_{DF}(L_F)^2\right) - 1\right)} + \varepsilon_1 \\
&= \sqrt{\rho^2 + \left(\rho(L_F)^3\left(1 + 2\rho L_{DF}(L_F)^2\right)\right)^2 - 2\rho\left(\rho(L_F)^3\left(1 + 2\rho L_{DF}(L_F)^2\right)\right)\sqrt{1-(\varepsilon_2)^2}} \\
&\quad + \varepsilon_1 \\
&= \rho\sqrt{1 + (L_F)^6\left(1 + 2\rho L_{DF}(L_F)^2\right)^2 - 2(L_F)^3\left(1 + 2\rho L_{DF}(L_F)^2\right)\sqrt{1-(\varepsilon_2)^2}} + \varepsilon_1.
\end{aligned}$$

Because both $f(\delta)$ and the bound (7) are monotone in ρ, and ρ is bounded by the radius r of the bounding sphere $S(r)$, we conclude that

$$\begin{aligned}
&|c - c'| \\
&\leq 2r\sqrt{1 + (L_F)^6\left(1 + 4rL_{DF}(L_F)^2\right)^2 - 2(L_F)^3\left(1 + 4rL_{DF}(L_F)^2\right)\sqrt{1-(\varepsilon_2)^2}} + \varepsilon_1.
\end{aligned} \tag{8}$$

For every point c in $\mathrm{ax}(\mathcal{S})$ we have found a point c' in $\overline{\mathrm{ax}(F(\mathcal{S}))}$ whose distance is bounded by (8), and therefore the one-sided Hausdorff distance between the two medial

axes $\mathrm{ax}(\mathcal{S})$ and $\overline{\mathrm{ax}(F(\mathcal{S}))}$ is bounded by the same quantity. Because the symmetrical formulation of the statement, the same bound holds for the Hausdorff distance. □

It was a surprise to the authors that no assumption on the set (apart from closedness) needed to be made, and that the techniques used were that simple and well established; they go back to Federer [1]. In fact, the authors at first envisioned a far more elaborate argument assuming the set had positive μ-reach [47].

4 Quantifying $C^{1,1}$ diffeomorphisms as deviations from identity

In this section we reformulate the main result in terms of norms on Banach spaces. This reformulation offers a more theoretical insight, and we believe the reformulated bounds are easier to work with in certain applications. Indeed, in the context of practical numerical computations, a bound on the Lipschitz constant of an operator — or, at least, a modulus of continuity — allows to control the condition number. This control is particularly useful when we calculate with objects such as the medial axis, whose (numerical) stability is often problematic in practice.

As we will see below, for this reformulation we somewhat strengthen our assumptions.

We decompose a diffeomorphism F into the identity map $\mathbb{1}_{\mathbb{R}^d}$ on $\mathbb{R}^d$, and a displacement field φ: $F = \mathbb{1}_{\mathbb{R}^d} + \varphi$. For the choice of the displacement field, we restrict ourselves to the vector space $\mathcal{U}$ of all $C^{1,1}$ maps φ from $\mathbb{R}^d$ to $\mathbb{R}^d$ whose restriction to the exterior $\mathbb{R}^d \setminus B(r)$ of a certain bounding ball $B(r)$ equals 0.[4]

A natural norm associated to $\mathcal{U}$ is one that makes it a Banach space. A typical choice, inherited from general Banach spaces of $C^{1,1}$ functions, would be for example, for $\varphi \in \mathcal{U}$,

$$\|\varphi\|_{C^{1,1}} = \max\left(\|\varphi\|_\infty, \|D\varphi\|_\infty, \mathrm{Lip}(D\varphi)\right). \tag{9}$$

Here we used the following notation:

- $\|\varphi\|_\infty = \sup_{x\in\mathbb{R}^d} |\varphi(x)|$ denotes the sup norm on $x \mapsto |\varphi(x)|$, where $|\cdot|$ is the Euclidean norm in $\mathbb{R}^d$,
- $\|D\varphi\|_\infty = \sup_{x\in\mathbb{R}^d} \|D\varphi(x)\|$ denotes the sup norm on $x \mapsto \|D\varphi(x)\|$, where $\|D\varphi(x)\|$ is the operator norm induced by the Euclidean norm on $\mathbb{R}^d$.
- We write $\mathrm{Lip}(D\varphi)$ for the Lipschitz semi-norm of $D\varphi$. The Lipschitz semi-norms of φ and $D\varphi$ are defined as

$$\mathrm{Lip}(\varphi) = \sup_{x,y\in\mathbb{R}^d,\, x\neq y} \frac{|\varphi(y) - \varphi(x)|}{|y - x|},$$

and

$$\mathrm{Lip}(D\varphi) = \sup_{x,y\in\mathbb{R}^d,\, x\neq y} \frac{\|D\varphi(y) - D\varphi(x)\|}{|y - x|}.$$

[4] This is more restrictive than assuming that the restriction to the bounding sphere $S(r)$ is 0, but it simplifies matters in this section.

The norm defined in (9) makes $\mathcal{U}$ into a Banach space, since every Cauchy sequence in $\mathcal{U}$ has a limit in $\mathcal{U}$. In addition, any function $\varphi \in \mathcal{U}$ satisfies:

$$\mathrm{Lip}(\varphi) = \|D\varphi\|_\infty, \tag{10}$$

$$\|D\varphi\|_\infty \leq r\,\mathrm{Lip}(D\varphi), \tag{11}$$

$$\|\varphi\|_\infty \leq r\,\mathrm{Lip}(\varphi) \leq r^2\,\mathrm{Lip}(D\varphi), \tag{12}$$

since the restriction of φ to $\mathbb{R}^d \backslash B(r)$ is 0. This in turn yields that $\mathrm{Lip}(D\varphi) \leq \|\varphi\|_{C^{1,1}} \leq \max(1, r, r^2)\,\mathrm{Lip}(D\varphi)$. Thus, in $\mathcal{U}$, the norm $\varphi \mapsto \mathrm{Lip}(D\varphi)$ is equivalent to the norm $\varphi \mapsto \|\varphi\|_{C^{1,1}}$.

We can now state slightly less general version of Theorem 18 in terms of the Banach space $(\mathcal{U},\ \varphi \mapsto \mathrm{Lip}(D\varphi))$.

Theorem 19. *Let $\mathcal{S} \subseteq \mathbb{R}^d$ be bounded by the ball $B(r)$ of radius $r > 0$, such that $S(r) = \partial B(r) \subseteq \mathcal{S}$. Let further F be a $C^{1,1}$ diffeomorphism from $\mathbb{R}^d$ to itself that leaves the set $\mathbb{R}^d \setminus B(r)$ invariant, and define two displacement fields $\varphi, \tilde{\varphi} \in \mathcal{U}$ such that $F = \mathbb{1}_{\mathbb{R}^d} + \varphi$ and*

$$(\mathbb{1}_{\mathbb{R}^d} + \tilde{\varphi}) \circ (\mathbb{1}_{\mathbb{R}^d} + \varphi) = \mathbb{1}_{\mathbb{R}^d}.$$

Define $\varepsilon = \max(\mathrm{Lip}(D\varphi), \mathrm{Lip}(D\tilde{\varphi}))$.

If $r\varepsilon \leq 1/4$, the Hausdorff distance between the medial axes of the set $\mathcal{S}$ and its image $F(\mathcal{S})$ is bounded by $d_H(\mathrm{ax}(\mathcal{S}), \mathrm{ax}(F(\mathcal{S}))) \leq \left(1 + \sqrt{50}\right) r^2\varepsilon + \mathcal{O}\left(r^3\varepsilon^2\right)$. In particular, $d_H(\mathrm{ax}(\mathcal{S}), \mathrm{ax}(F(\mathcal{S}))) = \mathcal{O}\left(r^2\varepsilon\right)$.

Proof. We denote $L_\varphi = \mathrm{Lip}(\phi)$. Expressions (5), (6) and (7) of the main article yield:

$$L_\varphi \leq r\varepsilon, \qquad L_{DF} = \varepsilon, \qquad L_F \leq 1 + L_\varphi \leq 1 + r\varepsilon, \qquad \varepsilon_1 \leq r^2\varepsilon, \qquad \varepsilon_2 \leq r\varepsilon. \tag{13}$$

We deduce

$$r\varepsilon \leq 1/4 \Longrightarrow r\varepsilon(1 + r\varepsilon)^2 \leq 1/2 \Longrightarrow rL_{DF}(L_F)^2 \leq 1/2.$$

Thus, the conditions of Theorem 18 are satisfied. Next, we reformulate the inequality (4) of Theorem 18. The expression E under the square root at the right hand side of this inequality is:

$$E = 1 + (L_F)^6 \left(1 + 4rL_{DF}(L_F)^2\right)^2 - 2(L_F)^3 \left(1 + 4rL_{DF}(L_F)^2\right) \sqrt{1 - (\varepsilon_2)^2}.$$

By replacing L_F by $1 + L_\varphi$ in E, the constants, as well as the degree-one terms in L_φ, rL_{DF}, and ε_2, cancel out. More precisely,

$$E = 16r^2L_{DF}^2 + r^2\varepsilon_2^2 + 24rL_\varphi L_{DF} + 9L_\varphi^2 + \mathcal{O}(|(rL_{DF}, L_\varphi, \varepsilon_2)|^3). \tag{14}$$

Finally, by substituting inequalities (13) into (14), we obtain

$$E \leq 50r^2\varepsilon^2 + \mathcal{O}\left(r^3\varepsilon^3\right),$$

and

$$d_H(\mathrm{ax}(\mathcal{S}), \mathrm{ax}(F(\mathcal{S}))) \leq \left(1 + \sqrt{50}\right) r^2\varepsilon + \mathcal{O}\left(r^3\varepsilon^2\right).$$

□

Remark 20. *Observe that the bound $\mathcal{O}\left(r^2\varepsilon\right)$ is consistent with a scaling by factor λ: $\mathcal{S} \mapsto \lambda\mathcal{S}$, $F(\cdot) \mapsto \lambda F(\cdot/\lambda)$. Under such a scaling, the radius r is multiplied by λ, while the Lipschitz constant $\mathrm{Lip}(D\varphi)$ — and therefore ε — is divided by λ. Furthermore, the Hausdorff distance $d_H(\mathrm{ax}(\mathcal{S}), \mathrm{ax}(F(\mathcal{S})))$ increases by a factor λ. By considering a diffeomorphism that translates the set $\mathcal{S} \setminus S(r)$ while keeping the bounding sphere $S(r)$ fixed, we see that this bound is asymptotically optimal.*

5 Conclusion and future work

We proved the Hausdorff stability of the medial axis of a closed set without any further assumption on it (as explained in Remark 1, the existence of the bounding sphere serves to formulate the main result in a clean way).

With regard to applications, our result is the first step towards providing a provably correct image recognition in the context of numerous scientific disciplines, and in particular of astrophysics. The next step is to produce physics-informed models for the medial axis as occurring in astronomical data.

On the mathematical side, we conclude with a conjecture generalizing our result to compact Riemannian manifolds with bounded curvature.

Conjecture 21. *Let $\mathcal{M}$ be a compact Riemannian manifold with bounded sectional curvature*[5] *and $\mathcal{S}$ a closed subset of $\mathcal{M}$. Then the medial axis (also called cut locus [49]) of $\mathcal{S}$ in $\mathcal{M}$ is Lipschitz stable under diffeomorphisms of $\mathcal{M}$.*

Acknowledgments

We are greatly indebted to Fred Chazal for sharing his insights. We further thank Erin Chambers, Christopher Fillmore, and Elizabeth Stephenson for early discussions and all members of the Edelsbrunner group (Institute of Science and Technology Austria) and the Datashape team (Inria) for the atmosphere in which this research was conducted.

Funding

The first author was supported by the European Union's Horizon 2020 research and innovation programme under the Marie Skłodowska-Curie grant agreement No. 754411 and the Austrian science fund (FWF) grant No. M-3073. This research has been supported by the European Research Council (ERC), grant No. 788183, by the Wittgenstein Prize, Austrian Science Fund (FWF), grant No. Z 342-N31, and by the DFG Collaborative Research Center TRR 109, Austrian Science Fund (FWF), grant No. I 02979-N35.

[5] See [48] for definitions and a very pedagogical overview of the properties of these manifolds.

Conflicts of interest/competing interests

None.

Ethical approval

Not applicable.

Availability of data and materials

Not applicable, i.e. no (synthetic) data was collected (generated).

References

[1] Federer, H.: Curvature measures. Transactions of the America mathematical Society **93**, 418–491 (1959)

[2] Amenta, N., Bern, M.: Surface reconstruction by Voronoi filtering. Discrete & Computational Geometry **22**(4), 481–504 (1999) https://doi.org/10.1007/PL00009475

[3] Chazal, F., Soufflet, R.: Stability and finiteness properties of medial axis and skeleton. Journal of Dynamical and Control Systems **10**(2), 149–170 (2004) https://doi.org/10.1023/B:JODS.0000024119.38784.ff

[4] Blaschke, W.: Kreis und Kugel. Verlag von Veit und Comp., Leipzig (1916)

[5] Attali, D., Boissonnat, J.-D., Edelsbrunner, H.: Stability and computation of medial axes - a state-of-the-art report. In: Möller, T., Hamann, B., Russell, R.D. (eds.) Mathematical Foundations of Scientific Visualization, Computer Graphics, and Massive Data Exploration, pp. 109–125. Springer, Berlin, Heidelberg (2009). https://doi.org/10.1007/b106657_6 . https://doi.org/10.1007/b106657_6

[6] Lieutier, A.: Any open bounded subset of $\mathbb{R}^n$ has the same homotopy type as its medial axis. Computer-Aided Design **36**(11), 1029–1046 (2004) https://doi.org/10.1016/j.cad.2004.01.011 . Solid Modeling Theory and Applications

[7] Mather, J.N.: Distance from a submanifold in Euclidean space. In: Proceedings of Symposia in Pure Mathematics, vol. 40, pp. 199–216 (1983). American Mathematical Society

[8] Thom, R.: Sur le cut-locus d'une variété plongée. Journal of Differential Geometry **6**(4), 577–586 (1972) https://doi.org/10.4310/jdg/1214430644

[9] Manen, M.: Maxwell strata and caustics. In: Brasselet, J.-P., Damon, J., Tráng, L.D.u., Oka, M. (eds.) Singularities in Geometry and Topology. Proceedings of the

Trieste Singularity Summer School and Workshop, pp. 787–824. World Scientific, ICTP, Trieste, Italy (2007)

[10] Wolter, F.-E.: Cut locus and medial axis in global shape interrogation and representation (1993)

[11] Damon, J.: Rigidity properties of the blum medial axis. Journal of Mathematical Imaging and Vision **63**(1), 120–129 (2021)

[12] Damon, J.: In: Siddiqi, K., Pizer, S.M. (eds.) Geometry and Medial Structure, pp. 69–123. Springer, Dordrecht (2008). https://doi.org/10.1007/978-1-4020-8658-8_3 . https://doi.org/10.1007/978-1-4020-8658-8_3

[13] Damon, J., Gasparovic, E.: Medial/skeletal Linking Structures for Multi-region Configurations. Memoirs of the American Mathematical Society, vol. 250. American Mathematical Society, Providence, Rhode Island (2017)

[14] Gasparovic, E.: The blum medial linking structure for multi-region analysis. PhD thesis, The University of North Carolina at Chapel Hill (2012)

[15] Wall, C.T.C.: Geometric properties of generic differentiable manifolds. In: Palis, J., Carmo, M. (eds.) Geometry and Topology, pp. 707–774. Springer, Berlin, Heidelberg (1977)

[16] Attali, D., Montanvert, A.: Computing and simplifying 2d and 3d continuous skeletons. Computer vision and image understanding **67**(3), 261–273 (1997)

[17] Chazal, F., Lieutier, A.: The λ-medial axis. Graphical Models **67**(4), 304–331 (2005)

[18] Lieutier, A., Wintraecken, M.: Hausdorff and gromov-hausdorff stable subsets of the medial axis. Proceedings of the 55th ACM Symposium on Theory of Computing (STOC 2023) (2023) arXiv:2303.04014

[19] Latombe, J.-C.: Robot Motion Planning. The Springer International Series in Engineering and Computer Science, vol. 124. Springer, New York (2012). https://doi.org/10.1007/978-1-4615-4022-9

[20] Amenta, N., Choi, S., Kolluri, R.K.: The power crust. In: Proceedings of the Sixth ACM Symposium on Solid Modeling and Applications, pp. 249–266 (2001)

[21] Tagliasacchi, A., Delame, T., Spagnuolo, M., Amenta, N., Telea, A.: 3d skeletons: A state-of-the-art report. In: Computer Graphics Forum, vol. 35, pp. 573–597 (2016). Wiley Online Library

[22] Hung, C.-C., Carlson, E.T., Connor, C.E.: Medial axis shape coding in macaque inferotemporal cortex. Neuron **74**(6), 1099–1113 (2012)

[23] Lescroart, M.D., Biederman, I.: Cortical representation of medial axis structure. Cerebral cortex **23**(3), 629–637 (2013)

[24] Chambers, E., Gasparovic, E., Leonard, K.: Medial fragments for segmentation of articulating objects in images. Research in Shape Analysis: WiSH2, Sirince, Turkey, June 2016, 1–15 (2018)

[25] Ho, S.-B., Dyer, C.R.: Shape smoothing using medial axis properties. IEEE Transactions on Pattern Analysis and Machine Intelligence **PAMI-8**(4), 512–520 (1986) https://doi.org/10.1109/TPAMI.1986.4767815

[26] Shaked, D., Bruckstein, A.M.: Pruning medial axes. Computer Vision and Image Understanding **69**(2), 156–169 (1998) https://doi.org/10.1006/cviu.1997.0598

[27] Demir, I., Hahn, C., Leonard, K., Morin, G., Rahbani, D., Panotopoulou, A., Fondevilla, A., Balashova, E., Durix, B., Kortylewski, A.: SkelNetOn 2019: Dataset and challenge on deep learning for geometric shape understanding. In: 2019 IEEE/CVF Conference on Computer Vision and Pattern Recognition Workshops (CVPRW), pp. 1143–1151 (2019). https://doi.org/10.1109/CVPRW.2019.00149

[28] Yan, Y., Sykes, K., Chambers, E., Letscher, D., Ju, T.: Erosion thickness on medial axes of 3d shapes. ACM Transactions on Graphics **35**(4), 38–13812 (2016) https://doi.org/10.1145/2897824.2925938

[29] Trinh, N.H., Kimia, B.B.: Skeleton search: Category-specific object recognition and segmentation using a skeletal shape model. International Journal of Computer Vision **94**, 215–240 (2011)

[30] Hu, J., Wang, B., Qian, L., Pan, Y., Guo, X., Liu, L., Wang, W.: MAT-Net: Medial axis transform network for 3D object recognition. In: International Joint Conference on Artificial Intelligence, pp. 774–781 (2019). https://doi.org/10.24963/ijcai.2019/109

[31] Rezanejad, M., Downs, G., Wilder, J., Walther, D.B., Jepson, A., Dickinson, S., Siddiqi, K.: Scene categorization from contours: Medial axis based salience measures. In: Proceedings of the IEEE/CVF Conference on Computer Vision and Pattern Recognition, pp. 4116–4124 (2019)

[32] Saha, P.K., Borgefors, G., Baja, G.S.: A survey on skeletonization algorithms and their applications. Pattern recognition letters **76**, 3–12 (2016)

[33] Aamari, E., Knop, A.: Statistical query complexity of manifold estimation. In: Proceedings of the 53rd Annual ACM SIGACT Symposium on Theory of Computing. STOC 2021, pp. 116–122. Association for Computing Machinery, New York, NY, USA (2021). https://doi.org/10.1145/3406325.3451135 . https://doi.org/10.1145/3406325.3451135

[34] Aamari, E., Levrard, C.: Stability and minimax optimality of tangential Delaunay complexes for manifold reconstruction. Discrete & Computational Geometry **59**, 923–971 (2018)

[35] Fefferman, C., Ivanov, S., Kurylev, Y., Lassas, M., Narayanan, H.: Fitting a putative manifold to noisy data. In: Conference On Learning Theory, pp. 688–720 (2018). PMLR

[36] Fefferman, C., Ivanov, S., Lassas, M., Narayanan, H.: Fitting a manifold of large reach to noisy data. arXiv preprint arXiv:1910.05084 (2019)

[37] Fefferman, C., Ivanov, S., Lassas, M., Narayanan, H.: Reconstruction of a Riemannian manifold from noisy intrinsic distances. SIAM Journal on Mathematics of Data Science **2**(3), 770–808 (2020)

[38] Sober, B., Levin, D.: Manifold approximation by moving least-squares projection (MMLS). Constructive Approximation **52**(3), 433–478 (2020)

[39] Fernie, J.D.: The period-luminosity relation: A historical review. Publications of the Astronomical Society of the Pacific **81**(483), 707 (1969) https://doi.org/10.1086/128847

[40] Peebles, P.J.E.: Principles of Physical Cosmology vol. 27. Princeton university press, Princeton (1993)

[41] Coble, K., McLin, K., Cominsky, L.: Big Ideas in Cosmology. Libretexts Physics, UC Davis (online) (2020)

[42] Bartelmann, M.: Gravitational lensing. Classical and Quantum Gravity **27**(23), 233001 (2010) https://doi.org/10.1088/0264-9381/27/23/233001

[43] Tang, Z., Von Gioi, R.G., Monasse, P., Morel, J.-M.: A precision analysis of camera distortion models. IEEE Transactions on Image Processing **26**(6), 2694–2704 (2017)

[44] Erdős, P.: Some remarks on the measurability of certain sets. Bulletin of the American Mathematical Society **51**(10), 728–731 (1945)

[45] Erdös, P.: On the Hausdorff dimension of some sets in Euclidean space. Bulletin of the American Mathematical Society **52**(2), 107–109 (1946) https://doi.org/bams/1183507696

[46] Blum, H.: A Transformation for Extracting New Descriptors of Shape. In: Wathen-Dunn, W. (ed.) Models for the Perception of Speech and Visual Form, pp. 362–380. MIT Press, Cambridge (1967)

[47] Chazal, F., Cohen-Steiner, D., Lieutier, A.: A sampling theory for compact sets in Euclidean space. Discrete and Computational Geometry **41**(3), 461–479 (2009)

[48] Berger, M.: A Panoramic View of Riemannian Geometry. Springer, Berlin, Heidelberg (2003). https://doi.org/10.1007/978-3-642-18245-7

[49] Kapovitch, V., Lytchak, A.: Remarks on manifolds with two-sided curvature bounds. Analysis and Geometry in Metric Spaces **9**(1), 53–64 (2021)

A Proofs of the Claims

Proof of Claim 16. Since any invertible matrix A satisfies $(A^t)^{-1} = (A^{-1})^t$, one has:

$$\begin{aligned} w \in D_pF(u^\perp) &\iff \langle D_pF^{-1}(w), u\rangle = 0 \\ &\iff \langle w, (D_pF^{-1})^t u\rangle = 0 \\ &\iff \langle w, u'\rangle = 0 \\ &\iff w \in u'^\perp, \end{aligned}$$

and thus

$$D_pF(u^\perp) = u'^\perp. \tag{15}$$

In other words, we have shown that u' is orthogonal to $D_pF(u^\perp) = D_pF(T)$.

Because

$$\langle D_pF(u), (D_pF^{-1})^t(u)\rangle = \langle D_pF^{-1}(D_pF(u)), u\rangle = \langle u, u\rangle > 0,$$

we deduce that $\langle D_pF(u), u'\rangle > 0$. This is in turn equivalent to u' pointing towards the interior of $F(B(c,\rho))$. □

Proof of Claim 17. We first show that $\angle u, u' < \pi/2$. Indeed, define the vector w as

$$w = (D_pF^t)^{-1}(u),$$

that is, the vector satisfying $u = D_pF^t(w)$. Then $u' = \frac{w}{|w|}$ (see equation (2)), and

$$\begin{aligned} |w|\langle u, u'\rangle = \langle u, w\rangle &= \langle D_pF^t w, w\rangle \\ &= \langle w, D_pFw\rangle = |w|^2 + \langle w, (D_pF - \mathrm{Id})w\rangle \\ &\geq |w|^2 - |w|^2 \,\|D_pF - \mathrm{Id}\,\| \\ &> 0. \qquad \text{(because, by assumption, } \|DF_p - \mathrm{Id}\,\| < 1) \end{aligned}$$

Thus, $\langle u, u'\rangle > 0$, and therefore $\angle u, u' < \pi/2$.

Furthermore, consider a vector $v \in u^\perp$. Since $\|v - D_pF(v)\| \leq \|D_pF - \mathrm{Id}\,\||v| \leq \varepsilon|v|$, the angle between v and $D_pF(v)$ is upper-bounded by $\arcsin\varepsilon < \pi/2$, as illustrated in Figure 6. This yields a bound on the angle between the tangent spaces $u^\perp$ and $D_pF(u^\perp)$:

$$\sin\angle u^\perp, D_pF(u^\perp) = \sin \sup_{v\in u^\perp, w\in D_pF(u^\perp)} \angle v, w \;\leq \varepsilon. \tag{16}$$

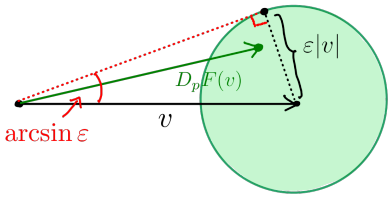

Fig. 6 Since $\|v - D_pF(v)\| \leq \varepsilon\,|v|$, the vector $D_pF(v)$ lies in the green ball $B(v, \varepsilon\,|v|)$. Since $\varepsilon < 1$, the angle between v and $D_pF(v)$ is upper-bounded by $\arcsin\varepsilon < \pi/2$.

Using (15) and (16) we deduce that:

$$\sin\angle u, u' = \sin\angle u^{\perp}, u'^{\perp} \leq \varepsilon.$$

Finally, since $\angle u, u' < \pi/2$, $\cos\angle u, u' \geq \sqrt{1-\varepsilon^2}$. This concludes the proof. □

B Federer's tubular neighbourhood lemma

We recall:

Lemma 22 (Federer's tubular neighbourhood lemma, Theorem 4.8 (12) of [1])**.** *Let $p \in \mathcal{S}$ and $\mathrm{lfs}(p) > 0$. The generalized normal space to $\mathcal{S}$ at p is characterized by the following property: For any $\rho \in \mathbb{R}$ satisfying $0 < \rho < \mathrm{lfs}(p)$,*

$$\mathrm{Nor}(p, \mathcal{S}) = \{\lambda v \in \mathbb{R}^d \mid \lambda \geq 0, |v| = \rho, \pi_{\mathcal{S}}(p+v) = \{p\}\}.$$

In particular, $\mathrm{Nor}(p, \mathcal{S})$ is a convex cone. The generalized tangent space $\mathrm{Tan}(p, \mathcal{S})$ is the convex cone dual to $\mathrm{Nor}(p, \mathcal{S})$.